

# A MICROMACHINED THERMAL FIELD-FLOW FRACTIONATION SYSTEM ( $\mu$ -TFFF)

Thayne L. Edwards<sup>1</sup>, Bruce K. Gale<sup>1</sup>, A. Bruno Frazier<sup>1,2</sup>

Departments of <sup>1</sup>Bioengineering and <sup>2</sup>Electrical Engineering

50 S. Central Campus Drive, Room 2480, University of Utah, Salt Lake City, Utah 84112

Phone: (801) 581-8611, Fax: (801) 585-5361, E-mail: Thayne.Edwards@m.cc.utah.edu

## ABSTRACT

In this work, a micro-scale thermal field-flow fractionation ( $\mu$ -TFFF) system has been designed, fabricated and characterized. TFFF systems are used for separation of biological and synthetic materials with different molecular weights as well as colloidal particles such as cells and proteins. Miniaturization of conventional macro-scale TFFF systems is made possible through utilization of micromachining technologies. Fabrication of the  $\mu$ -TFFF system is discussed in detail. Miniaturization of the TFFF system has the advantages of reduced sample size, reduced power consumption, and decreased analysis time for equivalent results. The effects of miniaturization on the performance of the  $\mu$ -TFFF system are compared with previous macro-scale TFFF systems and a previously fabricated micromachined electrical field-flow fractionation ( $\mu$ -EFFF) system [1]. Basic TFFF theory is discussed with respect to separation resolution and the advantages of miniaturization.

## INTRODUCTION

TFFF is an elution separation technique similar to chromatography except the separation field is normal, to the sample and carrier flow. TFFF utilizes thermal diffusion as the separation field instead of the gel, liquid, or column packing found in chromatographic separations. This field is accomplished by a temperature gradient across the channel. A schematic of the TFFF system is shown in Figure 1. Separation of suspended particles are performed in a solvent carrier such as methanol, THF, acetonitrile, or DMSO. Many solvents have been used and there have been studies

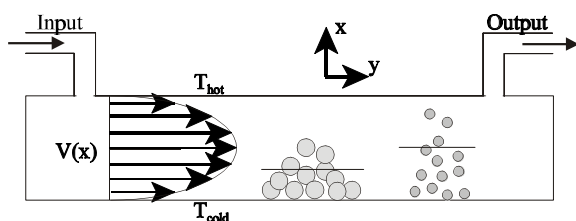


**Figure 1.** Schematic of a thermal field-flow fractionation (TFFF) channel. A temperature drop is held across the channel. The carrier velocity profile is laminar. These two factors lead to the separation of various sized particles.

shown how these solvents affect separation characteristics [2]. Water is not typically used as a carrier fluid unless an electrolyte has been added. The particles react to the temperature gradient by diffusing toward the cold wall. Higher molecular weight particles react more to the thermal gradient and are compacted more tightly against the cold wall than do lower molecular weight particles. Attempts have been made to understand and predict thermal diffusion [3]. Thermal diffusion is still not well understood. Because of the laminar velocity profile of the carrier, samples that compact less will have a higher average velocity than the samples that compact more. The difference in average velocity results in the spatial and temporal particle separation at the output of the TFFF channel.

The TFFF system has some unique characteristics making it more suitable for some separations than conventional system. In TFFF, the separation field is applied normal to the separation. The resolution requirement in the direction of separation is no longer needed, which means lower field strength, lower power consumption demands, and shorter separation times. TFFF also has the advantage of elution techniques, in that the samples are collected in fractions at given times. As a result, very pure samples can be obtained.

The theory of retention in TFFF has been well developed despite the lack of understanding thermal diffusion mechanisms. These exact mathematical relationships mean an elution sample volume can be related to physical parameters such as molecular weight, polydispersity, or the thermal diffusion coefficient [1]. Thus, TFFF can be used as an analysis tool as well as a separation device.

Speed and elution, as in chromatography, are combined with well developed theory and gentleness, as in centrifugation, in TFFF to give it a unique versatility in separations and analysis of both biological and synthetic materials.

## THEORY

In order for a separation in a TFFF channel to occur, there must be a difference in molecular weight or diameter of the components, a sample selective perturbation of the samples toward one wall, and a laminar velocity profile that results in a different average velocity of each constituent of a given sample. The channel of the TFFF system is typically

rectangular with a breadth to height ratio of greater than 100, which approximates infinite parallel plates. High aspect ratio channel cross sections are needed in order to neglect channel wall effects in the height direction.

In TFFF, samples are perturbed toward one wall by a thermal gradient. The migration of the particles toward the cold wall is a result of thermal diffusion and is represented by Equation 1.

$$J_{thermal} \approx D_T \frac{\Delta T}{w} c(x) = U c(x) \quad (1)$$

Here,  $D_T$  is the sample thermal diffusion coefficient and is strictly empirical sample dependent property.  $\Delta T/w$  is the  $x$ -direction thermal gradient  $U$  is the drift velocity of the particles. [4,5]

Concentration of the sample toward the cold wall results in a driving force for Fickian diffusion toward the hot wall. In Equation 2, the particle flux toward the hot wall,  $J$ , is a function of the particle diffusivity,  $D$ , and concentration gradient,  $dc/dx$ .

$$J = -D \frac{dc}{dx} \quad (2)$$

At equilibrium these opposing fluxes result in an exponential concentration gradient that is given by Equation 3.

$$c(x) = c_0 \exp\left(-\frac{x}{l}\right) \quad (3)$$

The concentration profile of the resulting thickness,  $l$ , of the sample layer. This thickness can also be represented by the dimensionless parameter,  $\lambda$ , which is defined as the fraction of the channel occupied by the sample ( $\lambda = l/w$ ). [4] The thickness,  $l$ , is a ratio of the diffusion coefficient,  $D$ , mentioned earlier, and the drift velocity of the particles,  $U$ , due to the applied field.

The drift velocity,  $U$ , is proportional to the flux from thermal diffusion, Equation 1. The result is that the thickness of the layer,  $\lambda$ , is directly related to the sample specific thermal diffusion coefficient,  $D_T$ . This approximated relationship is given by Equation 4. [4]

$$\lambda \approx \frac{D}{D_T \Delta T} \quad (4)$$

Several assumptions have been made to yield the relationship in Equation 4. First the thermal gradient is assumed to be constant across the channel. Second, because a thermal gradient is applied across the channel in the  $x$ -direction the viscosity of the fluid becomes dependent on  $x$  as well. The viscosity is typically assumed to be constant throughout the channel. However, there has been research into the effects of this position dependent viscosity on separations.

Another assumption made is that the solutes are

much smaller than the channel width. If the diameter of a solute is large, the effective velocity of the solute is higher than would be predicted. This effect has been implemented in size-exclusion FFF. [4]

The effect of the laminar velocity profile on a sample that occupies a specific fraction of the channel,  $\lambda$ , is to retain the sample in the channel longer. Retention is related to  $\lambda$  by equation 5.

$$R = 6\lambda \left[ \coth \frac{1}{2} \lambda - 2\lambda \right] = \frac{V_0}{V_r} \quad (5)$$

Retention is also determined experimentally by the ratio of the unretained volume (void volume),  $V_0$ , to the retained volume,  $V_r$ . Because time is related to the volumes of fluid by the flow rate, the ratio of void time,  $t_0$ , to retained time,  $t_r$ , is equivalent. [4]

Resolution is the degree of separation (overlap) between two samples at the end of the channel. The resolution is characterized by a resolution index,  $Rs$ . Equation 6 gives the resolution index as a function of channel length,  $L$ , relative molecular weight difference,  $\Delta M/M$ , the selectivity,  $S_M$ , and the plate height,  $H$ .

$$Rs = \frac{\sqrt{L}}{4} \frac{\Delta M}{M} \frac{S_M}{\sqrt{H}} \quad (6)$$

The selectivity of the thermal field toward a specific sample is given by Equation 7.

$$S = 3 \left( \frac{R}{36\lambda^2} + 1 - \frac{1}{\lambda} \right) S_{max} \quad (7)$$

$S_{max}$  is a system dependent parameter that varies between 0.33 and 0.80. [4] Plate height,  $H$ , represents the width or spreading of a sample peak during separation. The plate height is a function of the instrument and operation, polydispersity of the sample, and non-equilibrium effects as given by Equation 8.

$$H = H_n + \sum H_i + H_p \quad (8)$$

The instrument term,  $H_i$ , can be minimized through extremely smooth surfaces and good channel geometry control, both are of which are possible with micromachining. The non-equilibrium,  $H_n$ , is effected by this reduction in channel height,  $w$ , as is seen in Equation 9.

$$H_n \approx 24\lambda^3 w^2 \frac{\langle v \rangle}{D} \quad (9)$$

$D$  is the diffusivity,  $v$  is the velocity, and  $\lambda$ , is the sample layer thickness. [4]

The resolution index,  $Rs$ , can be determined from the physical and operating parameters of the instrument and the samples by using Equations 4, 5, 7, and 9 in Equation 8, which result is given by Equation 10.

$$Rs \approx \frac{3 S_{max} \left( \frac{\Delta M}{M} \right)}{8 w D} \sqrt{\frac{L D_T^3 \Delta T^3}{6 \langle v \rangle}} \quad (10)$$

From Equation 10 it can be seen that the resolution is inversely proportional to the channel width,  $w$ . By decreasing  $w$ , the resolution increases. As a result, for a given separation, the resolution time is shorter, or, for a given time the resolution is higher. Micromachining techniques are available to reduce this channel width to dimensions that macromachining techniques are not capable of. [1,4]

## EXPERIMENTAL METHODS

### Fabrication

The  $\mu$ -TFFF system was fabricated with an n-type, [100], single side polished, silicon wafer using common micromachining processes. The final wafer would contain ten  $\mu$ -TFFF channels of varying widths (2.0mm - 6.0mm) and lengths ( 4.0cm - 6.0cm). A silicon dioxide ( $\text{SiO}_2$ ) mask was thermally grown at  $900^\circ\text{C}$  to approximately  $1\mu\text{m}$  thick. Photolithographic techniques were used to define the input/output ports in the photoresist on the back side of the wafer. The  $\text{SiO}_2$  mask was etched using a buffered HF solution. The ports were then anisotropically etched through the silicon wafer in 20% KOH at  $55^\circ\text{C}$ .

The  $\text{SiO}_2$  was then used as the mask for the boron diffused heaters. Patterning the  $\text{SiO}_2$  was accomplished using the same method as for the ports. Boron was then diffused at  $1175^\circ\text{C}$  to a depth of  $5\mu\text{m}$  at a concentration of approximately  $4 \times 10^{20}\text{cm}^{-3}$ . These parameters estimate a resistivity of  $9 \times 10^{-4}\Omega\text{-cm}$ .

A negative photosensitive polymer (SU-8) was spun on to a thickness of  $25\mu\text{m}$  onto the wafer. The channels were defined in the SU-8 by UV exposure and developing. Heat treatment of the channel walls ensured a strong bond and durability when exposed to the carrier fluid, which is typically an organic solvent.

A glass microscope slide was affixed to the top of the SU-8 to complete the channel, shown in Figure 2. The adhesive was required to withstand both thermal and chemical degradation and not increase the channel height significantly.

After completing the fabrication of the  $\mu$ -TFFF separation channel, the complete system was assembled (e.g. fluid interconnections, power supply, flow meters, and detector) and tested as shown in Figure 3. Adhesive for the interconnects were required to be mechanically strong as well as withstand the thermal and chemical attacks described for adhesion of the glass slide to the walls.

### Test Procedure

Using the  $\mu$ -TFFF device fabricated as described in this paper, the total plate height,  $H$ , was determined as a function of flow rate for an unretained sample. DI water was used as the carrier and pure acetone was used as the sample. The flow rate of water was set by the pump. The flow rates used were 2.34, 1.5, 1.0, 0.6,

and 0.3 mL/hr. An acetone sample,  $0.1\mu\text{L}$ , was injected into the input port at time zero for each flow rate. A detector measured the absorbance with respect to a sample of DI water. Data were collected with a PC.

## RESULTS

One end of a fabricated channel and port is shown in Figure 4a. The channel height has been reduced from  $127\mu\text{m}$  (macro-TFFF system) [5] to  $50\mu\text{m}$  ( $\mu$ -TFFF). The resistance of the boron diffused heaters were measured to be  $3\text{-}12\Omega$  depending upon the length and width of the heater. These resistances were used to calculate a resistivity of  $3 \pm 1 \times 10^{-4}\Omega\text{-cm}$ . A power of only 10 W was required to achieve a  $20^\circ\text{C}$  temperature difference across the channel. This is more than 10 times lower than that reported for a typical macro-scale TFFF channel [5]. The completed  $\mu$ -TFFF system is shown in Figure 4b where the system is ready for operation.

Detector response for a  $1\mu\text{L}$  unretained pure acetone sample is plotted in Figure 5a. The flow rate of the water carrier was  $1\text{mL}/\text{min}$ . The elution time is 117 seconds with 5.7 theoretical plates. Plate height,  $H$ , was determined as a function of average carrier velocity and compared with results from the  $\mu$ -EFFF system [1] and TFFF theoretical results. The plate height curve is shown in Figure 5b. The  $\mu$ -TFFF plate height characteristics follow the curves that are found in the  $\mu$ -EFFF channel as well as the theoretical curve for the TFFF system. The data are of the nearly same magnitude or lower than the sum of plate heights

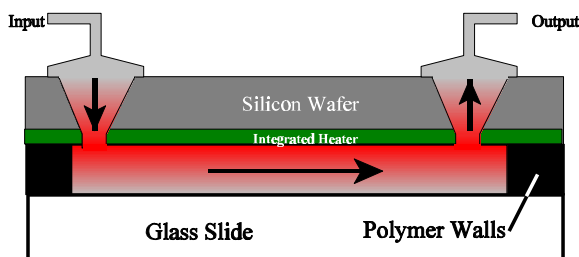


**Figure 2.** Layout of a micro-thermal field-flow fractionation channel ( $\mu$ -TFFF). The temperature gradient is maintained using an integrated, boron doped, heater.

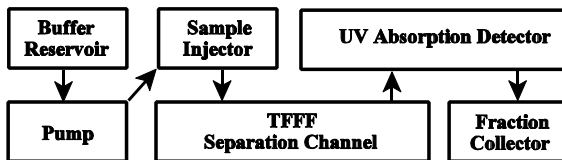


**Figure 3.** Flow diagram of a completed  $\mu$ -TFFF separation system.

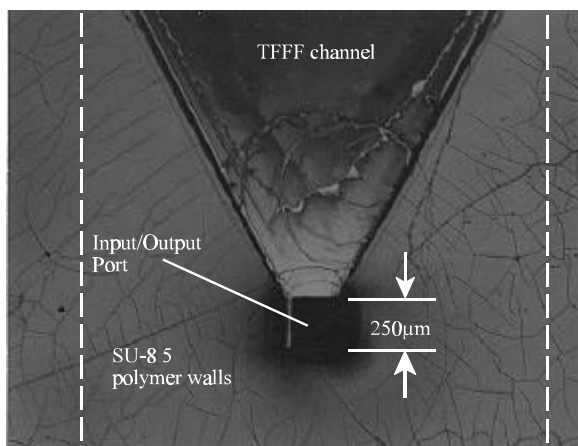


**Figure 4a.** Photograph of fabricated channel and etched port. Surrounding area is SU-8 (24.6 $\mu$ m). The heater region is between the two dashed lines.

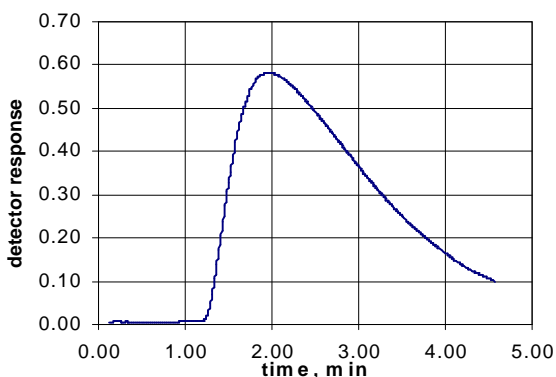


**Figure 5a.** Response of the detector to a 0.1 $\mu$ L acetone sample in a water carrier. The flow was set to 1mL/hr.

reported for retained polystyrene samples ( $MW_n$ : 154k, 392k, and 735k). The temperature gradient was 30 $^{\circ}$ C and toluene is the carrier. The dimension of the channel is 0.025cm  $\times$  1.2 cm  $\times$  305cm. [6]

### CONCLUSION

A micromachined thermal field-flow fractionation device has been successfully fabricated and tested. Fabrication techniques common to micromachining were implemented with excellent quality and control of the channel geometry and reduced the dimensions of the channel beyond that which conventional macro-machining processes are incapable of achieving. These techniques also allowed for an integrated heater which power consumption was decreased by a factor of over 10 over common conventional TFFF systems. The  $\mu$ -TFFF system exhibited plate height attributes similar to those from the  $\mu$ -EFFF system, macro-TFFF system, and theory.

### ACKNOWLEDGMENTS

The authors would like to thank MicroChem Corp. and the Whitaker foundation project support.

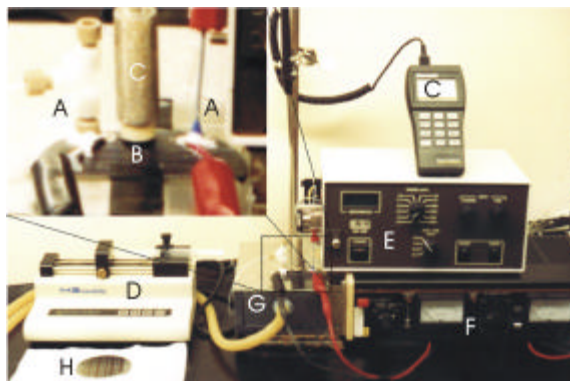


**Figure 4b.** Photograph of complete  $\mu$ -TFFF system, including (A) interconnects, (B) completed device (C) thermometer, (D) pump, (E) detector, (F) power supply, and (G) heat sink, (H) fabricated channels on wafer.

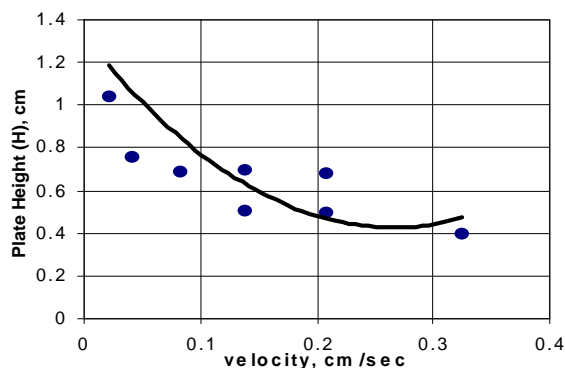


**Figure 5b.** Plate height for unretained sample. Carrier-DI water, sample-0.1 $\mu$ L 100% acetone. Curve is similar to the TFFF theoretical and  $\mu$ -EFFF channel curves.

### REFERENCES

- [1] Gale, B.K., Frazier, A.B., Caldwell, K.D., *Characterization of a  $\mu$ -EFFF system*, MEMS '97, pp. 119-124.
- [2] Sisson, R.M., Giddings, J.C. Nov. 15, 1994. *Effects of solvent composition on polymer retention in TFFF*. Analytical Chem., 66, pp. 4043-4053.
- [3] Rue, C.A., Schimpf, M.E. Nov. 15, 1994. *Thermal diffusion in liquid mixtures and its effect on polymer retention in thermal field-flow fractionation*. Analytical Chem., 66, pp. 4054-4062.
- [4] Caldwell, K.D. 1987. *Field-flow fractionation of biological materials*. Dept. of Bioengineering, University of Utah.
- [5] Lou, J.Z. March 1994. *Studies on the theory and applications of polymer separation by thermal field-flow fractionation*. Ph.D. Thesis, University of Utah, Salt Lake City, Utah. p. 37.
- [6] Hovingh, M.E., Thompson, G.H., Giddings, J.C. Feb. 1970. *Column parameters in TFFF*. Analytical chem., 42, pp. 195-1203.